Proceedings of the 21st ICSMGE, Vienna, Austria, 14 – 19 June 2026. Pistrol, Adam & Schweiger (eds.)
Published by: ÖGG, Austrian Society for Geomechanics, Salzburg, Austria, ISBN 978-3-9503898-4-5
https://doi.org/10.53243/ICSMGE2026-963

Advancing Safety Risk Assessment in Subsea Tunnel Excavation: A Digital Twin Framework Integrating Computer Vision and Material Point Method

Mingliang Zhou, Jie Xu, Zeyu Li, Qihao Jiang, Dongming Zhang, Hongwei Huang
Department of Geotechnical Engineering, College of Civil Engineering, Tongji University, Shanghai, China,
zhoum@tongji.edu.cn

ABSTRACT: Subsea tunnel excavation through water-rich fault zones faces heightened safety risks due to geological complexity and high permeability, often resulting in water inrush and face collapse hazards. To address these challenges, this study develops an innovative digital twin framework that integrates a computer vision–based spatial monitoring with Material Point Method (MPM) simulations for comprehensive safety risk assessment. Real-time personnel distribution is captured and processed, while geological properties are derived from computer vision-based approach, and modeled probabilistically via lognormal distributions to capture geological uncertainty. The resulting geological model is feed into a two-phase double-point MPM model that simulates coupled fluid–solid interactions and collapse scenarios in fault zones. The framework quantitatively estimates collapse probabilities, spatial influence ranges, and associated risks to personnel, schedule, and economic outcomes. Results show that casualty risks are strongly linked to worker distribution during specific construction stages, while economic losses are primarily driven by casualty compensation and delay-related costs. This scalable, data-informed approach offers a rapid and accurate decision-support tool for managing safety risks in complex subsea tunneling projects and can be extended to other underground engineering contexts with challenging geological and safety conditions.

KEYWORDS: Subsea tunnel excavation, Digital twin, Material Point Method, Risk assessment, Computer vision

1 INTRODUCTION

The rapid expansion of subsea tunnelling toward greater depths, longer alignments, and increasingly large cross-sections has exposed projects to highly heterogeneous and unpredictable geological environments. Subsea rock masses are dominated by pervasive jointing, fracturing, and water-rich structural planes, whose strong spatial variability and degraded mechanical properties can induce sudden deformation, instability, collapse, or water inrush during excavation. However, despite these escalating hazards, existing risk assessment methods remain fundamentally limited: they lack real-time adaptability to overcome highly uncertain geological changes, provide no physics-based quantification of collapse likelihood, and offer only coarse or qualitative estimates of potential casualties, economic losses, or schedule disruptions. As a result, subsea tunnelling still lacks a rigorous, dynamic, and quantitative framework capable of supporting operational safety decisions during excavation.

Accurate characterization of geological strata is essential for ensuring excavation stability. However, traditional geotechnical investigations rely on sparse borehole data that cannot capture the complex, small-scale heterogeneity of subsea rock masses along long tunnel alignments. Recent advances in computer vision and deep learning have enabled high-resolution extraction of fractures, weak zones, and lithological boundaries directly from tunnel face imagery, providing essential spatial detail for real-time geological modelling. When combined with advanced numerical simulation, these data open new opportunities to reconstruct local geological conditions and predict potential failure mechanisms at the excavation face.

Numerical modelling has played a central role in analysing tunnel face stability, particularly when geological discontinuities are involved (Xu et al., 2011; Liu et al., 2014; Liang et al., 2023; Zheng et al., 2011). However, most conventional finite-element or limit-equilibrium studies assume small deformations and are unable to reproduce progressive face collapse or coupled deformation–seepage failure processes commonly observed in practice. The Material Point Method (MPM) has emerged as a powerful alternative for modelling large-deformation geomechanics, offering improved numerical stability by tracking state variables on material points rather than grids. Its accuracy has been validated against centrifuge tests and physical model experiments (Kafaji et al., 2013; Cheng et al., 2015; Elliot, 2019; Fernández et al., 2021; Li et al., 2023), making it particularly suited for simulating collapse and water inrush in fractured, water-rich environments. Liang et al. (2020) used a two-phase, two-set-material-point approach to assess dike stability under overtopping flows, Du et al. (2022) simulated landslide-induced surge chains, and Zhao et al. (2022) modelled granular-landslide-generated tsunamis. However, most existing applications have focused on seepage-induced slope or dike failure with deterministic simulations, without embedding uncertainty quantification or connecting failure outcomes to risk metrics such as losses or excavation delays.

Risk assessment for subsea tunnels intersecting water-rich faults has advanced through multi-indicator frameworks such as AHP–Cloud models (Peng, 2020) and Bayesian networks (Wang et al., 2022), which integrate empirical data with engineering case validation. However, these methods remain largely qualitative, rely on expert scoring or empirical probabilities, and are not designed for dynamic, cycle-by-cycle assessment during drill-and-blast subsea tunnel excavation. These studies lack physics-based modelling of progressive collapse, resulting in an absence of quantitative loss estimation essential for supporting excavation-stage operational decisions.

This study addresses the aforementioned gaps by introducing a digital twin framework for predictive, excavation-stage risk assessment in subsea tunnels advancing through water-rich fractured rock masses. The proposed framework integrates computer vision–driven geological perception, probabilistic tunnel face failure analysis, and multidimensional loss quantification supported by two-phase MPM simulations. By linking simulated collapse scales to personnel exposure, repair timelines, and cost impacts, it provides quantitative estimates of casualty, schedule, and economic risks at the operational level. The framework is demonstrated through its application to the Qingdao Jiaozhou Bay Second Subsea Tunnel, where geological features such as fractures, leakage pathways, and lithological boundaries are automatically extracted from high-resolution imagery and incorporated into physics-based simulations of progressive failure. By integrating real-time geological sensing, uncertainty-aware numerical modelling, and quantitative impact assessment, this work establishes a new

paradigm for subsea tunnel safety evaluation, enabling excavation-cycle decision support and transitioning practice from reactive response to proactive risk mitigation.

2 THE DIGITAL TWIN FRAMEWORK

2.1 *Computer vision-based geological model reconstruction*

In subsea tunnelling, complex stratigraphy (e.g. multiple fracture sets, lithological interfaces, and weak zones) creates significant safety risks during excavation. Robust 3D geological models are therefore required to delineate formation boundaries and provide defensible inputs for numerical modelling and risk evaluation. Conventional investigations along subsea alignments yield sparse, point-wise data, and isolated boreholes rarely capture the strong spatial heterogeneity of the subsurface. A 3D spatial transition probability matrix was established using all borehole unit data as conditional constraints, enabling the reconstruction of the geological uncertainty of 3D formations. In addition, a spatial deep learning model is proposed to conduct 3D geological model inference via face image sequences This innovative approach incorporates multimodal field data, including geological investigation report, borehole logs, drilling observations, tunnel face imagery (Figure 1). The resultant 3D geological models effectively visualize and characterize the spatial distributions of diverse rock and soil types, significantly enhancing the ability to segment and interpret geological features at different tunnel cross-sections.

To enable dynamic updating of the 3D geological model during excavation, high-resolution cameras are deployed after each blasting and mucking cycle to capture multi-angle images of the tunnel face and surrounding rock. In parallel, geological sketches are prepared to record key attributes, including leakage conditions, fracture orientation (strike, dip, dip angle), filling thickness, and lithology. These datasets are processed using the developed computer vision–based deep learning pipeline (Zhou et al., 2021; Chen et al., 2021; Wu et al., 2023). Leakage detection is performed using an enhanced GAN–Swin Transformer network (Wu et al., 2023), which classifies, localises, and visualises water inflow patterns directly within the 3D model. Fracture mapping is achieved with the FraSegNet model (Chen et al., 2021), which integrates multi-scale feature extraction modules (e.g., ASPP) and boundary refinement (e.g., guided filtering) to achieve pixel-level segmentation of complex fracture networks. The segmentation output is then refined via skeleton extraction to produce single-pixel-width fracture centerlines. Key node coordinates are derived using chain-code tracing and polyline approximation, enabling automated calculation of structural plane orientation and spatial positioning of weak zones. These parameters are exported as chain-code coordinate files for direct integration into the geological model (Figure 2).

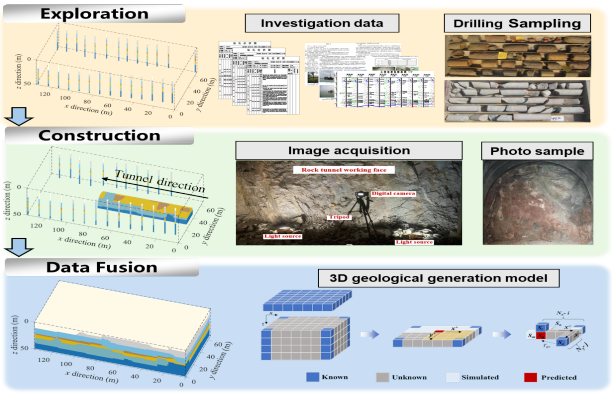

Figure 1. Schematic Diagram of the Proposed 3D Geological Model Reconstruction Process

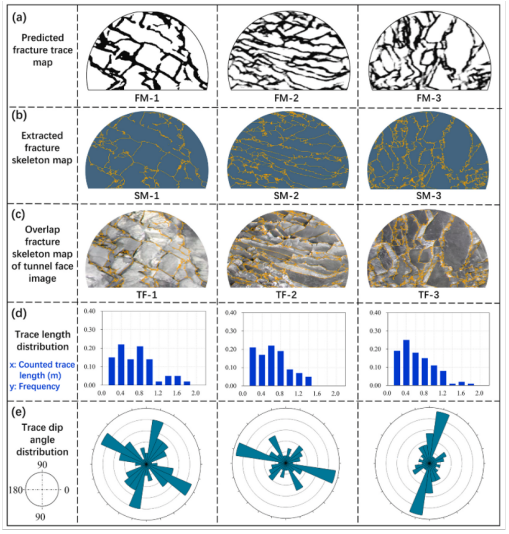

Figure 2. Key Feature Extraction and Quantification via Computer Vision and Deep Learning

2.2 *MPM simulation for failure influence range evaluation*

The reconstructed geological model is subsequently embedded into a s two-phase double-point Material Point Method (MPM) modeling framework, capable of simulating complex fluid-solid interactions encountered during subsea tunnel excavation. The mesh size of the numerical model depending on both the acquired data resolution and the numerical computational needs. The MPM framework integrates coupled solid-fluid behavior equations with advanced constitutive models specifically tailored to the geomechanical characteristics of subsea fault zones. This integration accounts for critical factors such as rock permeability, water viscosity, and tunnel geometry. Through detailed simulations, the model effectively captures the dynamic evolution of fluid flow velocities, pore water pressure distributions, and face failure trajectories within fractured zones ahead of excavation fronts, thus providing critical insights into water influx dynamics (Figure 3). An integrated CAD-GiD-MPM workflow was developed to address ongoing challenges associated with high-fidelity 3D geological modelling. Utilizing DXF interfaces, the model geometry is transferred into GiD, leveraging its advanced meshing capabilities to produce accurate material point clouds. This integrated approach enables efficient numerical model generation for simulating the water inrush-induced collapse problem.

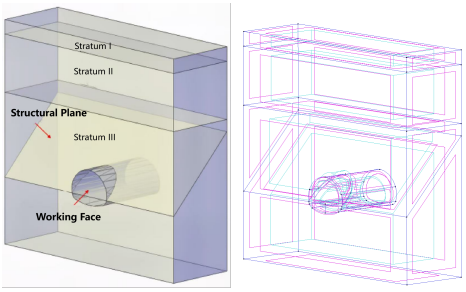

Figure 3. CAD-Drawn 3D Stratigraphic Diagram and GiD 3D Image.

It is widely recognized that subsea tunnel face failure is governed by coupled hydro-mechanical processes. In numerical modelling, seepage fields are commonly represented as liquid-phase water flow using fluid mechanics parameters such as drag force, viscosity, and hydraulic pressure. Alternatively, seepage can be characterized via the rock mass permeability coefficient,

which incorporates the effects of hydraulic pressure, water velocity, and porosity. In this study, a seepage-induced failure model is adopted to explicitly distinguish between solid and liquid phases, enabling more accurate simulation of their respective motion states. This model, originally developed and integrated into the MPM software Anura3D by Ceccato et al. (2016), and has been applied in various contexts. It incorporates the interaction between solid and liquid phases by considering factors such as rock mass permeability, water viscosity, and tunnel geometry. This approach allow the simulation to reflect the changes in liquid phase flow velocity, pore water pressure, and particle trajectories in the fractured zone ahead of the working face after the fracture zone is exposed, revealing the dynamic evolution of water influx following excavation.

3 TUNNEL EXCAVATION RISK ASSESSMENT

The risk assessment for tunnel excavation was carried out by integrating the hydro-mechanical failure analysis and the reconstructed geological model from Section 2 with on-site construction activity data. Specifically, the calculated influence ranges of water inrush and collapse were integrated with the spatio-temporal distribution of personnel and machinery throughout the excavation process (Figure 4). Analysis of the evolution curves for effective porosity, permeability coefficient, and cementation degree revealed that water inrush influence zones are primarily controlled by permeability and porosity, whereas collapse deformation zones are jointly governed by mechanical properties and permeability characteristics. To capture parameter uncertainty, Latin Hypercube Sampling (LHS) was performed to generate a comprehensive disaster scenario database, from which the corresponding failure influence ranges were derived. Exceedance probability curves for different impact extents were then established, enabling quantitative evaluation of event probabilities. Finally, detailed on-site surveys provided accurate mapping of personnel and machinery distributions at various construction stages, supporting loss quantification and overall risk assessment.

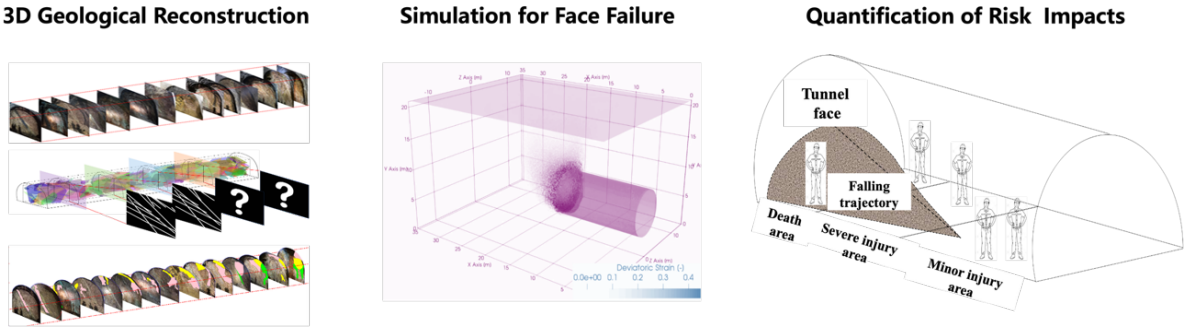

Figure 4. Integrated Risk Evaluation Approach.

3.1 *Risk probability evaluation*

In this study, risk probability is defined as the exceedance probability that the maximum propagation distance of the solid–liquid slump mass within the tunnel face surpasses a specified threshold, accounting for the uncertainty in surrounding rock geological parameters. To ensure the reliability of the computed exceedance probabilities and maintain a low coefficient of variation (COV), a sufficiently large number of parameter realizations must be analyzed. For example, when the expected exceedance probability is on the order of 10^{-2}, a total sample size M must exceed 10,000 to achieve a COV below 0.1. Accordingly, LHS was adopted to generate 10,000 representative combinations of geological parameters, from which the exceedance probability curves for face failure influence ranges were derived.

Subsequently, Material Point Method (MPM) simulations were performed to determine face failure influence ranges under varying combinations of geological parameters. For each simulated scenario involving water inrush or collapse, the farthest post-excavation movement distance of the solid–liquid mixture relative to the working face was extracted and defined as the face failure influence range. Exceedance probability analyses were then applied to these results, quantifying the likelihood that tunnel water inrush or collapse would extend beyond specified distances. This probability framework was further integrated with on-site personnel and machinery distribution data, enabling quantitative estimation of the occurrence probabilities for different risk levels and the corresponding potential losses in terms of casualties, schedule delays, and economic impacts.

To investigate the displacement characteristics of water inrush and collapse in the unexcavated fault rock mass behind the working face after a tunnel intersects a water-rich fault, a numerical model simulating tunnel excavation through a vertical water-rich fault was developed (Figure 5). For 10,000 simulations, the 3D geological model was simplified to a two-dimensional configuration under the plane strain assumption. The model measures 67.5 m in length, with a 7.5 m-thick saturated fault fracture zone flanked on both sides by 30 m-thick sections of moderately weathered granite. The tunnel, 10 m in diameter and buried at a depth of 20 m, is excavated from within one granite section toward the fault. A 7.5 m-deep surface water body overlies the site. The fault fracture zone is simultated by the proposed Fault Cementation Constitutive Model (FCCS) in our previous work (Li et al., 2024), while the granite is characterized using the Mohr–Coulomb failure criterion. The liquid phase follows a Newtonian fluid model. Fully fixed constraints are applied at the bottom boundary, and roller constraints at the lateral boundaries, acting on both solid and liquid phases. After excavation, vertical constraints are imposed on the upper and lower boundaries of the excavated section to simulate activated support measures. For computational stability and efficiency, the numerical model mesh size is set to 1 m within the fault zone and tunnel section, and 2 m elsewhere, with each element containing 6 solid-phase material points (SMPs) and 6 liquid-phase material points (LMPs).

Regarding the model parameter selection, the physical and mechanical properties of both the moderately weathered granite and the fault fracture zone, such as density, porosity, permeability coefficient, and cohesion, are derived from the field geological investigation report to ensure realistic representation of in-situ conditions. For the water-rich fault zone, parameter ranges are established by defining upper and lower bounds based on measured geological data and relevant empirical correlations. To account for natural variability and

uncertainty, all parameters are assumed to follow a lognormal probability distribution and are treated as mutually independent in the random sampling process. These statistical assumptions facilitate probabilistic analyses across the 10,000 simulation cases. The complete set of variable ranges adopted in the model are summarized in Table 1.

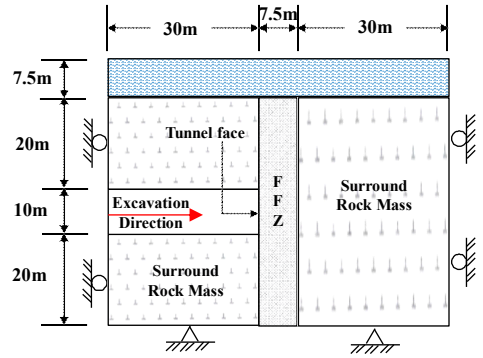

Figure 5. Schematic Diagram of Tunnel Excavation Model.

Based on actual construction conditions and detailed field investigations, this study statistically analyzes scenarios in which large deformations occur simultaneously in both the solid and liquid phases, namely, water inrush accompanied by collapse. The sensitivity of tunnel face deformation was analysed using multiple linear regression with eight parameters as independent variables. The solid-phase collapse range and liquid-phase water-influx range from seepage-induced failure simulations served as dependent variables. The critical state stress ratio (M), and cementation degree (X_c) show the strongest influence, confirming their dominant role in controlling rock-mass shear strength and collapse extent. Other parameters (κ, λ, a, c) have weaker but still meaningful effects through their influence on stiffness and hardening behaviour. In contrast, porosity (n) and intrinsic permeability (κ_L) strongly enlarges both collapse and water-influx ranges by increasing seepage pathways and weakening structural confinement. Intrinsic permeability directly enhances fluid mobility and can trigger changes in the failure mode once a threshold is exceeded.

After the tunnel excavation exposes the fault, the deformation and collapse of the rock mass led to the redistribution of porosity, resulting in an increase in permeability and a decrease in degree of cementation. The increase in permeability induced by rock mass collapse leads to accelerated water inflow, and the impact of the inflow can entrain the fractured rock mass to move with the water, affecting the stability of tunnel face, which is reflected by the degree of rock mass deformation and damage.

For tunnel face failure likelihood evaluation, the "failure impact range" is defined as the region containing 95% of the material points within the collapsed rock mass. The failure influence range, R, is measured as the distance from the leading edge of this main collapse mass to the tunnel working face and is extracted from 10,000 random parameter combination simulations. The exceedance probability, P, is then computed; for example, among the 10,000 cases, 227 cases exhibited R>5m and 45 cases exhibited R>10m, corresponding to P(R>5m) = 0.0227 and P(R>10m) = 0.0045. From these results, the exceedance probability curve of the collapse impact scope is plotted (Figure 6), showing a distinct linear decay in a double logarithmic coordinate system, indicative of a power-law relationship between collapse scope and exceedance probability. This pattern arises because large-scale collapses occur only when multiple key parameters—particularly rock mass strength and permeability—are simultaneously at extreme values. In most cases, higher rock mass strength and lower permeability effectively constrain the extent of collapse, resulting in smaller failure influence ranges.

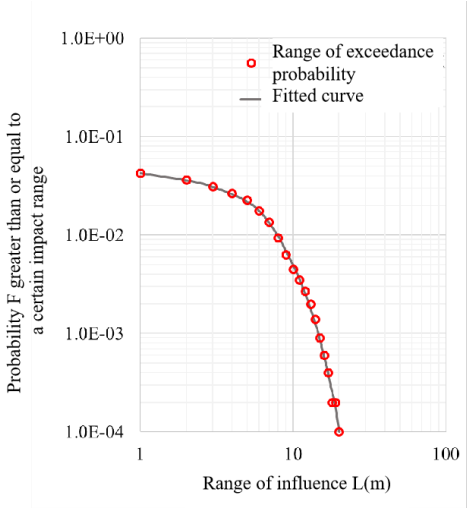

Figure 6. Exceedance Probability Curve for Different Impact Range.

Table 1. Parameter Sampling for Exceedance Probability Calculation Using Latin Hypercube Sampling

Parameter	Meaning	Value		
Parameters about fault skeleton		Lower limit	Upper limit	Increment
κ	Slope of a swelling line	0.001	0.03	0.001
λ	Slope of the normal compression line	0.03	0.3	0.01
$p0'$	Initial consolidation pressure /kPa	100	3000	100
M	Slope of critical state line	0.8	1.5	0.01
u	Sub-loading Constant	1	20	1
Parameters about fault cement				
Xc	Cement degree	0.01	0.5	0.01
m	Consolidation Shear Weakening Coefficient	0.5	1.5	0.1
a	Cohesion enhancement parameter /kPa	1000	5000	100
b	Cohesion enhancement coefficients		1	
c	Dilation enhancement parameter /kPa	100	300	10
d	Dilation enhancement coefficients		1	
m^2	Cement Shear Modulus Enhancement Parameter /kPa	1000	3000	100
Permeation-related parameters				
n	Porosity	0.1	0.5	0.01
K	Permeability m/d	0.1	5	0.1

3.2 *Quantitative Risk Loss Analysis*

In this study, risk losses were quantified across three key dimensions: personnel casualties, schedule delays, and economic impacts. Each construction cycle was divided into multiple stages, with high-risk activities identified as mucking, scaling, initial shotcreting, steel arch installation, rock bolting, and final shotcreting. The likelihood of disaster occurrence at each stage was weighted proportionally according to its duration within the overall construction cycle.

To achieve accurate estimation of losses following a working face collapse, a spatial–temporal distribution model was developed for personnel, equipment, and working cycles in the tunnel face area typical of subsea tunnel construction sites. This model, serving as the foundation for quantitative risk loss assessment, was constructed through a combination of field investigations at multiple drill-and-blast tunnels, interviews with construction managers, review of relevant engineering codes and standards, and expert questionnaires. Using this framework, quantitative risk indicators were calculated for working face collapse events across five critical high-risk stages: risk elimination, mucking, steel arch installation, rock bolting, and shotcreting. This integrated approach allows the assessment of potential casualties, delays, and economic losses in a probabilistic and scenario-based manner, directly linking the exceedance probabilities derived in Section 3.1 to quantitative risk assessment outcomes.

The quantitative risk associated with tunnel working face collapse can be expressed as the product of the probability of occurrence of a risk event and the resulting loss, as formulated by Knight (2013):

$$R = P_R * C_R \tag{1}$$

where, P_R represents the occurrence probability of a specific risk event, and C_R denotes the corresponding loss incurred.

Building on the approach of Li et al.(2014) and incorporating the spatio-temporal distribution of personnel across different construction stages, the Risk of Personnel Casualties (R_{PC})is defined as a quantitative risk indicator：

$$R_{PC} = P_R \times \sum (P_{P/R} \times P_{WS/R} \times V_{WS/R}) \tag{2}$$

For quantifying schedule delays caused by tunnel working face collapse, the Risk of Time Delay (R_{TD}) is established, integrating repair procedures and stage-specific durations：

$$R_{TD} = P_R \times \sum (T_{WR} + T_{EP} + T_{DC} + T_{RR} + T_C) \tag{3}$$

Similarly, the Risk of Economic Loss (R_{EL}) consolidates the above components along with other cost factors：

$$R_{TD} = P_R \times \sum (C_{WC} + C_{MD} + (C_{DC} + C_{RR} + C_{SC}) + C_{TD}) \tag{4}$$

Assuming the total exceedance probability of the solid–liquid mixture impact range exceeding a distance $L > n$ is $P(R > n)$, the total duration of high-risk stages is T_{total}, and the duration of a specific construction stage is T_i, the conditional probability of collapse occurrence with impact scope exceeding n during construction stage i is expressed by Equation (6):

$$P(R > n|i) = P(R > n) \times \frac{T_i}{T_{total}} \tag{5}$$

For example, for a collapse exceeding 5 meters (R>5m) during the 3-hour mucking stage, given $P(R > 5m) = 0.0227$. and T_{total} = 13 h, the conditional probability is calculated as:

$$P(R > 5m|mucking) = P(R > 5m) \times \frac{T_{mucking}}{T_{total}} = 0.0227 \times \frac{3}{13} = 0.005238 \tag{6}$$

Using these conditional probabilities, the exceedance probability and corresponding impact ranges of collapse events of different magnitudes can be calculated for each construction stage, linking critical nodes for personnel, schedule, and economic losses with the probabilistic outcomes of tunnel collapse. Finally, F–N (Frequency–Number of casualties) curve methodology is employed to represent the risks across three different aspects. Curves are generated to depict the F–N curve for personnel casualties, the F–TD curve for schedule delays, and the F–D curve for economic losses per construction stage (Figure 7), providing a comprehensive visualization of risk distribution throughout the construction process.

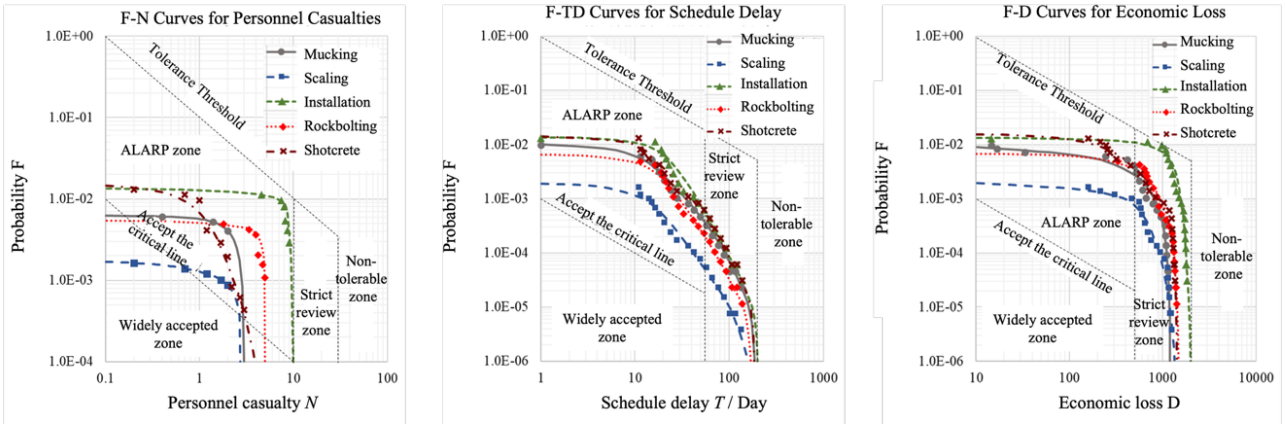

Figure 7. Risk Evaluation Curves for Personnel Casualty, Schedule Delay, and Economic Loss

The results shown in Figure 7 indicate that personnel casualty risk is highly sensitive to the spatial distribution of tunnel workers during different construction stages. In smaller-scale collapse/water inrush events, schedule delays are strongly correlated with the number of casualties, whereas in large-scale collapse/water inrush events, the primary drivers of delay are the extended durations required for debris removal, structural repair, and reinforcement. Economic losses are found to be dominated by compensation payments for casualties and the financial impact of schedule delays, with repair costs representing a smaller but non-negligible proportion.

4 CONCLUSIONS

This study advances safety risk assessment in subsea tunnel excavation by developing a digital twin framework that couples

computer vision–based ecvation face information with large-deformation Material Point Method (MPM) simulations. The framework integrates real-time personnel distribution, automatically extracted from video using computer vision, with probabilistic collapse simulations driven by field-derived geological parameters. By modelling uncertainties in porosity, permeability, and mechanical properties using lognormal distributions, the method captures the inherent variability of water-rich faulted rock masses with high fidelity.

The integrated approach enables fully quantitative evaluation of collapse probability, influence range, and associated risks to personnel, schedule, and project economics. The results show that casualty risk is highly dependent on worker positioning during different tunnel excavation stages; small-scale collapses primarily induce schedule delays, whereas large-scale failures are dominated by extended cleanup, repair, and reinforcement operations. Correspondingly, economic losses arise mainly from casualty compensation and delay-related costs.

The proposed framework accommodates wide parameter ranges and complex geological conditions typical of subsea tunnels, providing a practical and operationally relevant tool for engineering risk management. When excavation intersects a fault or unexpected weak zone, engineers can rapidly construct a 3D geological model, run probabilistic MPM simulations, and estimate collapse likelihood and spatial extent. By combining predicted failure zones with stage-specific personnel distribution statistics, the framework allows quantification of casualty probabilities. Collapse extent further informs cleanup and repair duration, enabling estimation of schedule delays and corresponding economic impacts

Overall, this digital twin framework provides a systematic, data-driven basis for predictive safety assessment during subsea tunnel excavation. It offers a significant improvement over traditional qualitative methods by supporting proactive decision-making, enabling rapid scenario analysis, and enhancing risk-informed construction management in highly uncertain geological environments.

5 REFERENCES

Xu, C., Xia, C., & Chen, X. (2011).Characteristics analyses of deformation and failure on tunnel surrounding rock based on fine description of joints. Chinese Journal of Rock Mechanics and Engineering,2011,30(10), 1997–2003.

Liu, X., Liu, W., & Suo, C. (2014).Effects of the joint dip angle on the collapsed arch of surrounding rock around a highway tunnel. Modern Tunnelling Technology,2014,51(06):73-77.

Liang, C., & Wang, Y. (2023).Research on the collapse law of tunnel surrounded with fracture rock under blasting load. Chinese Journal of Underground Space and Engineering,2023,19(05):1699-1707.

Zheng, Y., Wang, Y., Wang, C., et al. (2011).Stability analysis and exploration of failure law of jointed rock tunnel——Seminor on Tunnel Stability Analysis. Chinese Journal of Underground Space and Engineering,2011,7(04):649-656.

Kafaji, I.K.J.A. (2013). Formulation of a dynamic material point method (MPM) for geomechanical problems.

Cheng X, Zheng G, SOGA K, et al. Jie.Post-failure behavior of tunnel heading collapse by MPM simulation[J].Science China (Technological Sciences), 2015, 58(12), 2139-2152.

Elliot James Fern, Modelling tunnel-induced deformations with the material point method, Computers and Geotechnics, Volume 111, 202-208 (2019).

Fabricio Fernández, Jhonatan E.G. Rojas, Eurípedes A. Vargas, Raquel Q. Velloso, Daniel Dias: Three-dimensional face stability analysis of shallow tunnels using numerical limit analysis and material point method. Tunnelling and Underground Space Technology, Volume 112, 103904 (2021).

Li, Z., Huang, H., Zhou, M., & Zhang, D. (2023). Failure responses of rock tunnel faces during excavation through the fault-fracture zone. Underground Space,10(2023),pp.166-181.

Aiqing Wu, Wen Zhao. A detailed study of the CHN-BQ rock mass classification method and its correlations with RMR and Q system and Hoek-Brown criterion[J]. International Journal of Rock Mechanics and Mining Sciences, 2023, 162.

Peng K, Zhou J Q, Zou Q L, et al. Deformation characteristics and failure modes of sandstones under discontinuous multi-level cyclic loads [J]. Powder Technol, 2020, 373: 599-613.

Wang Y C, Liu Y, Li Z Y, et al. A New Bayesian Network Model for the Risk Assessment of Water Inrush in Karst Tunnels [J]. Geofluids, 2022, 2022.

Zhou, M., Chen, J., Huang, H., Zhang, D., Zhao, S. and Shadabfar, M., 2021. Multi-source data driven method for assessing the rock mass quality of a NATM tunnel face via hybrid ensemble learning models. International Journal of Rock Mechanics and Mining Sciences, 147, p.104914.

Chen, J., Zhou, M., Huang, H., Zhang, D. and Peng, Z.,2021. Automated extraction and evaluation of fracture trace maps from rock tunnel face images via deep learning. International Journal of Rock Mechanics and Mining Sciences,142, p.104745.

Wu, C., Huang, H., Zhang, L., Chen, J., Tong, Y. and Zhou, M., 2023. Towards automated 3D evaluation of water leakage on a tunnel face via improved GAN and self-attention DL model. Tunnelling and Underground Space Technology, 142, p.105432.

Ceccato F, Beuth L, Vermeer P A, et al. Two-phase material point method applied to the study of cone penetration [J]. Computers and Geotechnics, 2016, 80: 440-52.

Liang D F, Zhao X Y, Soga K. Simulation of overtopping and seepage induced dike failure using two-point MPM [J]. Soils and Foundations, 2020, 60(4): 978-88.

Du W J, Sheng Q, Fu X D, et al. A TPDP-MPM-based approach to understanding the evolution mechanism of landslide-induced disaster chain [J]. Journal of Rock Mechanics and Geotechnical Engineering, 2022, 14(4): 1200-9.

Zhao K-L, Qiu L-C, Liu Y. Two-layer two-phase material point method simulation of granular landslides and generated tsunami waves [J]. Physics of Fluids, 2022, 34(12).

Li Z, Zhou, ZHOU M, HUANG H, et al. Mechanical properties and constitutive characterization of fault gouge considering cementation effects [J]. Journal of Applied Basic and Engineering Science, 2024,32(06):1801-1819.

Knight F. Risk, Uncertainty and Profit [J]. Vernon Press Titles in Economics, 2013, (4): 682-90.

Li Z H, Huang H W, Xue Y D. Cut-slope versus shallow tunnel: Risk-based decision making framework for alternative selection [J]. Engineering Geology, 2014, 176: 11-23.

ACKNOWLEDGMENTS

This work is supported by the National Natural Science Foundation of China (No. 52522810, 52379106) and the CRSRI Open Research Program (CKWV20231174/KY).